

MARS 2020 PERSEVERANCE TRAJECTORY RECONSTRUCTION AND PERFORMANCE FROM LAUNCH THROUGH LANDING

Fernando Abilleira^{*}, Gerard Kruizinga[†], Seth Aaron[‡], Kris Ankasa[§], Todd Barber^{},
Paul Brugarolas^{††}, Dan Burkhart^{‡‡}, Al Chen^{§§}, Stuart Demcak^{***}, John Essmiller^{†††},
John Gilbert^{‡‡‡}, Eric Gustafson^{§§§}, Julie Kangas^{****}, Mark Jesick^{††††}, Sarah Elizabeth
McCandless^{‡‡‡}, Swati Mohan^{§§§§}, Neil Mottinger^{*****}, Clara O'Farrell^{†††††},
Richard Otero^{‡‡‡‡}, Christopher Pong^{§§§§§}, Mark Ryne^{*****}, Jill Seubert^{†††††},
Paul Thompson^{‡‡‡‡‡}, Sean Wagner^{§§§§§§}, Mau Wong^{*****}**

The Mars 2020 (M2020) Mission carrying Perseverance, the most advanced rover ever sent to Mars, successfully launched on an Atlas V 541 (AV-088) launch vehicle from the Eastern Test Range (ETR) at Cape Canaveral Air Force Station (CCAFS) in Florida at 11:50:00 UTC (T-Zero time) on July 30, 2020. After some station reconfiguration, carrier/telemetry were locked at both Deep Space Network (DSN) Canberra and Goldstone stations. Perseverance entered the Martian atmosphere at 20:36:50 Spacecraft Event Time (SCET) UTC, and landed inside Jezero Crater at 20:43:49 SCET UTC on February 18, 2021. Confirmation of nominal landing was received at the DSN Goldstone and Madrid tracking stations via the Mars Reconnaissance Orbiter at 20:55:11 Earth Received Time (ERT) UTC. This paper summarizes in detail the actual vs. predicted performance in terms of launch vehicle events, launch vehicle injection performance, actual DSN spacecraft lockup, trajectory correction maneuver performance, Entry, Descent, and Landing events, and overall trajectory and geometric characteristics.

INTRODUCTION

The successful landing of the Perseverance rover inside Jezero Crater carrying the most advanced scientific payload suite ever sent to the Red Planet has the potential of rewriting history books. The mission's scientific objectives include investigating Mars habitability and searching for bio signatures that may have

^{*} M2020 Mission Design and Navigation Manager and Deputy Mission Manager, Fernando.Abilleira@jpl.nasa.gov

[†] M2020 Navigation Team Chief, Gerhard.L.Kruizinga@jpl.nasa.gov

[‡] M2020 EDL Trajectory Analyst, Seth.Aaron@jpl.nasa.gov

[§] M2020 Mission Interface Manager (DSN), Krisjani.S.Ankasa@jpl.nasa.gov

^{**} M2020 Propulsion Lead, Todd.J.Barber@jpl.nasa.gov

^{††} M2020 GNC Chief Engineer, Paul.Brugarolas@jpl.nasa.gov

^{‡‡} M2020 EDL Trajectory Lead, Paul.D.Burkhart@jpl.nasa.gov

^{§§} M2020 EDL Manager, Allen.Chen@jpl.nasa.gov

^{***} M2020 Navigation Shift Lead and MAVEN Navigation Team Chief, sdemcak@jpl.nasa.gov

^{†††} M2020 Launch, Cruise Phase Lead, John.C.Essmiller@jpl.nasa.gov

^{‡‡‡} M2020 Mission Planner, John.B.Gilbert@jpl.nasa.gov

^{§§§} M2020 Orbit Determination Analyst, Eric.D.Gustafson-133274@jpl.nasa.gov

^{****} M2020 Trajectory Lead and Maneuver Analyst, Julie.A.Kangas@jpl.nasa.gov

^{††††} M2020 Orbit Determination Analyst, Maneuver Analyst, and Software Design Lead, Mark.C.Jesick@jpl.nasa.gov

^{‡‡‡‡} M2020 Orbit Determination Analyst, Sarah.E.McCandless@jpl.nasa.gov

^{§§§§} M2020 Guidance, Navigation & Control Operations Lead, Swati.Mohan@jpl.nasa.gov

^{*****} M2020 Orbit Determination Analyst, Neil.Mottinger@jpl.nasa.gov

^{†††††} M2020 EDL Trajectory Analyst, ofarrell@jpl.nasa.gov

^{‡‡‡‡‡} M2020 EDL Ops Lead and Council of Terrains Lead, Richard.E.Otero@jpl.nasa.gov

^{§§§§§} M2020 ACS Analyst, Christopher.M.Pong@jpl.nasa.gov

^{*****} M2020 Orbit Determination Analyst, Mark.S.Ryne@jpl.nasa.gov

^{††††††} M2020 Orbit Determination Lead, Tombasco@jpl.nasa.gov

^{‡‡‡‡‡‡} M2020 Navigation Shift Lead, Paul.F.Thompson@jpl.nasa.gov

^{§§§§§§} M2020 Maneuver Analyst and MRO Maneuver Lead, Sean.V.Wagner@jpl.nasa.gov

^{*****} M2020 Maneuver Lead, Mau.C.Wong@jpl.nasa.gov

been preserved in rocks which could serve as evidence of past microbial life¹. Something truly unique about this particular objective is that the most relevant samples will be cached and stored for their potential return to Earth by a future mission (not earlier than 2031). This is a key feature since any ground-breaking discoveries will require irrefutable evidence which would need to be confirmed by state-of-art laboratories on Earth. Perseverance will also characterize the Martian climate. The MEDA instrument will measure temperature, winds, pressure, humidity, and dust. Perseverance will also study the geological environment of the surface and the subsurface, and search for rocks which were formed in the presence of water. The rover also includes key experiments that will prepare us for future crewed missions to Mars such as the MOXIE experiment which will produce oxygen from Mars' carbon dioxide in the atmosphere.

The M2020 mass at launch was 4,061 kg, about 220 kg heavier than the Mars Science Laboratory (MSL) launch mass^{2,3}. The heavier launch mass was mostly due to the heavier rover (1,026 kg vs 899 kg of the MSL rover) and the additional weight of the strengthened supersonic parachute. Both flight systems had a small cruise propellant allocation of ~70 kg to maximize the payload mass to be delivered to Mars; hence, a nominal injection imparted by the launch vehicle, small maneuver execution errors, and precise orbit determination solutions were critical to precisely deliver the spacecraft to the optimal Mars atmospheric Entry Interface Point (EIP). M2020's excellent trans-Mars injection, maneuver performance, and orbit determination accuracy resulted in ample cruise propellant margins at Mars arrival. Interplanetary navigation and Entry, Descent, and Landing (EDL) performance were incredibly accurate and the third trajectory correction maneuver executed about two months prior to arriving to Mars was the last maneuver needed to meet delivery requirements. Good EDL attitude initialization, exceptional performance by the on-board entry guidance system and by the never-used-before Terrain Relative Navigation (TRN) system, and atmospheric uncertainties and winds within the expected levels, resulted in the successful and extremely precise landing of Perseverance only ~1.7 km southeast from the intended target. Figures 1 and 2 show some of the first iconic images that Perseverance sent back to Earth within a few hours after landing.



Figure 1. Rover view from the Skycrane during EDL



Figure 2. Perseverance's First Color Image

LAUNCH PERIOD AND LAUNCH/ARRIVAL STRATEGY

The original 30-day M2020 launch period extended from July 17, 2020 through August 15, 2020. The arrival date on February 18, 2021 was kept constant for all launch dates to simplify planning of surface operations⁴. This constant arrival date resulted in a small entry time variation of ~11 min across the launch period. Both the open and the close of the launch period were constrained by United Launch Alliance's (ULA) Atlas V 541 launch performance capability. At the open of launch period, the high Declination of the Launch Asymptote (DLA) had the largest impact on launch capability as the launch energy (C3) was near the lowest across the launch period. At the close of the launch period, declinations were low; however, C3 was the highest. During the launch vehicle target specification cycles with ULA, additional launch vehicle capability became available as launch vehicle flight performance reserves (FPR) held to ensure sufficient performance to achieve the trans-Mars injection and launch vehicle contingency (LVC) bookkept to account for vehicle design maturity, monthly effects, targeting bias, and final Centaur weighing were released. Also, the spacecraft mass launch mass uncertainty was reduced which resulted in additional launch capability. With this additional performance, the opening of the launch period could have been a few days earlier than July

17, 2020; however, the M2020 Project elected to protect the Assembly, Testing, and Launch Operations (ATLO) schedule margins and utilize the additional performance towards extending the duration of the daily launch windows whenever possible. In order to ensure DSN visibility at spacecraft transmitter on time, expected ~5 min after spacecraft separation, ULA's strategy for each individual daily launch window included launch window skewing techniques in conjunction with a 1 min spacecraft separation delay from the Centaur upper stage. This strategy ensured there would be no gaps in DSN communications. Launch and Mars arrival timings were also driven by UHF EDL communications via the Mars Reconnaissance Orbiter (MRO) and Mars Atmospheric and Volatile Evolution (MAVEN) along with X-band Direct-To-Earth communications⁵. The launch period was optimized to keep MRO's Local Mean Solar Time (LMST) node as close to possible to its nominal value of 2:52 PM (ascending) used to support InSight landing. In order to improve EDL communications, MRO executed an orbit correction maneuver (OCM-4) on December 12, 2018, two weeks after InSight EDL, to change the nodal drift such that 3:15 PM LMST would be achieved at M2020 EDL on February 18, 2021. After further analysis, the LMST target was updated to 3:30 PM LMST. This new target required the addition of OCM-4A which was executed on October 23, 2019. MAVEN executed an inclination change maneuver (ICM-1) on July 25, 2018 and used aerobraking from February 12, 2019 through April 4, 2019 to ensure the orbital plane was optimal for EDL comm support. Additional phasing maneuvers executed by both MRO and MAVEN were executed within a year from M2020 EDL to correct for any timing errors. Later arrival dates would have extended the duration of DTE X-band communications; however, for later arrival dates, MRO's LMST would have had to be shifted even later. An arrival on February 18, 2021 did not provide X-band DTE tones through touchdown; however, it provided full telemetry through landing by both MRO and MAVEN. As such, UHF relay was selected as the primary communications path and ensured a robust EDL communications strategy. X-band 8 kbps tones remained available through entry plus ~381 sec and served as a secondary communications path that was particularly useful during plasma blackout which the spacecraft experienced 35 sec after atmospheric entry for about a minute. During this blackout period and as expected, the UHF signal was lost but DTE X-band tones continued. Signal via the DTE link was lost as expected prior to landing due to antenna angle violations. The launch arrival strategy is shown on Figure 3.

Initially, delays in launch vehicle processing activities shifted the open of the launch period to July 23, 2020; however, on June 25, 2020, ULA and NASA's Launch Services Program (LSP) found a leak inside the liquid oxygen (LOX) tank of the Centaur. A few days later a weld void was identified visually. Weld repair and verification of the repair integrity were successful and the encapsulated assembly was transported to the vehicle integration facility and finally mated to the booster on July 7, 2020. This resulted in an additional delay to the open of the launch period to July 30, 2020 which further reduced the duration of the launch period to 17 launch days.

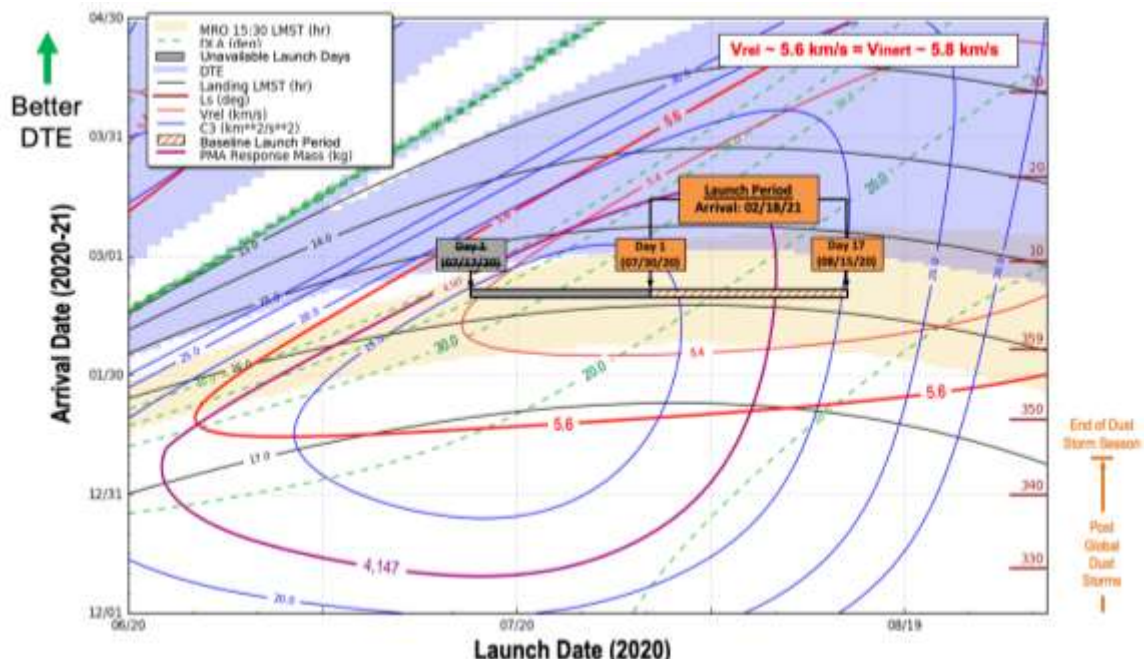


Figure 3. Launch/Arrival Strategy

LAUNCH WINDOWS AND LIFTOFF TIMES

The duration of the launch window was primarily determined by the variable Declination of the Launch Asymptote (DLA), a launch site (LSC-41) latitude of 28.42 deg, a fixed launch azimuth for each park orbit family (110.5 deg for launches from July 17, 2020 through July 23, 2020 and 96.0 deg for launches from July 24, 2020 through August 15), launch vehicle ascent trajectory capabilities, and available launch vehicle performance for which the launch vehicle could liftoff and deliver the spacecraft to the specified targets⁴. Due to operational constraints, the maximum daily launch window duration was constrained to 2 hours. The available propellant for the trans-Mars injection burn by the Centaur upper stage was limited by propellant reserves to account for lower-than-expected launch vehicle performance, launch vehicle weight uncertainties, and environmental variation effects. For M2020, Flight Performance Reserves (FPR) were 159 kg. Launch Vehicle Contingency (LVC) expendable propellant was kept at 159 kg.

For M2020, launch opportunities occurred every five minutes on the whole minute. The Right ascension of the Launch Asymptote (RLA) determined the actual liftoff time. All launch windows satisfied the requirement associated with a payload containing radioisotope materials for which a launch shall occur during civil twilight and Centaur mandatory telemetry coverage constraints.

The M2020 spacecraft carrying the Perseverance rover successfully launched on July 30, 2020 at 11:50 UTC (07:50 EDT/ 04:50 PDT) which corresponded to the launch window open time on launch day 1. Table 1 and Figure 4 provide the final launch times and launch windows for each day in the launch period⁶.

Table 1. Launch Windows, Launch Times, and Launch Duration

	Launch Day	Launch Date (2020, UTC)	Window Open (hh:mm, UTC)	Window Close (hh:mm, UTC)	Window Open (hh:mm, EDT)	Window Close (hh:mm, EDT)	Window Open (hh:mm, PDT)	Window Close (hh:mm, PDT)	Window Duration (hh:mm)	Number of Opp.
Launch Days eliminated due to delays in LV Readiness	-	07/17	13:00	14:45	09:00	10:45	06:00	07:45	01:45	22
	-	07/18	12:50	14:50	08:50	10:50	05:50	07:50	02:00	25
	-	07/19	12:55	14:55	08:55	10:55	05:55	07:55	02:00	25
	-	07/20	13:15	15:15	09:15	11:15	06:15	08:15	02:00	25
	-	07/21	13:30	15:30	09:30	11:30	06:30	08:30	02:00	25
	-	07/22	13:35	15:35	09:35	11:35	06:35	08:35	02:00	25
	-	07/23	13:40	15:40	09:40	11:40	06:40	08:40	02:00	25
	-	07/24	11:45	13:35	07:45	09:35	04:45	06:35	01:50	23
	-	07/25	11:35	13:35	07:35	09:35	04:35	06:35	02:00	25
	-	07/26	11:20	13:20	07:20	09:20	04:20	06:20	02:00	25
	-	07/27	11:30	13:30	07:30	09:30	04:30	06:30	02:00	25
	-	07/28	11:40	13:40	07:40	09:40	04:40	06:40	02:00	25
	-	07/29	11:45	13:45	07:45	09:45	04:45	06:45	02:00	25
Available Launch Days	1	07/30	11:50	13:50	07:50	09:50	04:50	06:50	02:00	25
	2	07/31	11:55	13:55	07:55	09:55	04:55	06:55	02:00	25
	3	08/01	11:55	13:55	07:55	09:55	04:55	06:55	02:00	25
	4	08/02	11:55	13:55	07:55	09:55	04:55	06:55	02:00	23
	5	08/03	12:00	13:55	08:00	09:55	05:00	06:55	01:55	24
	6	08/04	12:05	13:55	08:05	09:55	05:05	06:55	01:50	23
	7	08/05	12:10	13:50	08:10	09:50	05:10	06:50	01:40	21
	8	08/06	12:15	13:50	08:15	09:50	05:15	06:50	01:35	20
	9	08/07	12:20	13:45	08:20	09:45	05:20	06:45	01:25	18
	10	08/08	12:25	13:45	08:25	09:45	05:25	06:45	01:20	17
	11	08/09	12:35	13:45	08:35	09:45	05:35	06:45	01:10	15
	12	08/10	12:40	13:40	08:40	09:40	05:40	06:40	01:00	13
	13	08/11	12:45	13:35	08:45	09:35	05:45	06:35	00:50	11
	14	08/12	12:50	13:30	08:50	09:30	05:50	06:30	00:40	9
	15	08/13	12:55	13:25	08:55	09:25	05:55	06:25	00:30	7
	16	08/14	12:55	13:25	08:55	09:25	05:55	06:25	00:30	7
	17	08/15	12:55	13:25	08:55	09:25	05:55	06:25	00:30	7

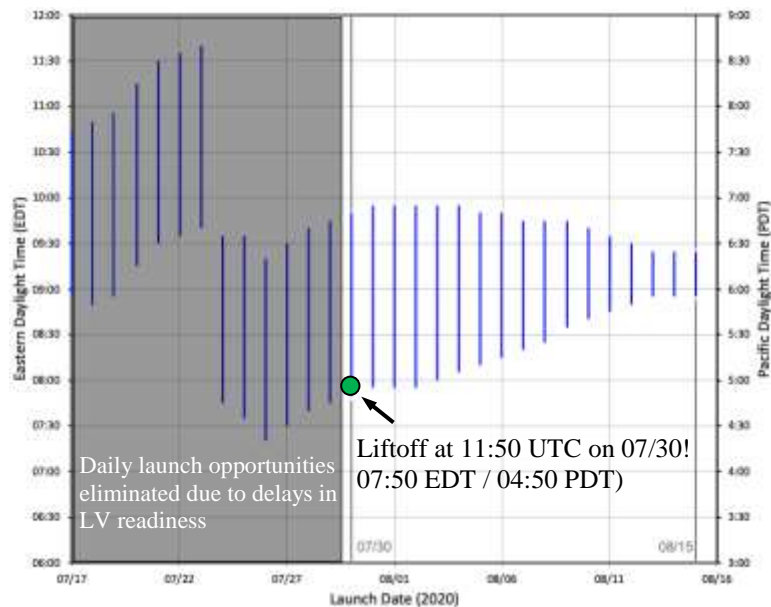


Figure 4. Launch Windows and Launch Times

LAUNCH VEHICLE EVENTS

On the ground, the RD-180 engine system (a single set of turbo machinery with 2 thrust chambers) was ignited to provide thrust for liftoff. At a fixed time from Go-Inertial, the four Solid Rocket Booster (SRBs) were also ignited. Liftoff occurred shortly thereafter. At approximately 80 sec into flight, the SRBs burned out and jettisoned. The Common Core Booster (CCB) flight continued in this closed-loop phase until sensors detected propellant depletion which occurred ~263 sec after liftoff. Centaur separation occurred ~6 seconds after Booster Engine Cutoff (BECO). Both Common Core Booster (CCB) ascent and Centaur separation were nominal. A nearly seven-minute burn by the Centaur put the spacecraft into the desired 167 x 250 km, 29.1 deg inclination parking orbit. After the ~33 min coasting period, a second burn of the Centaur RL-10 engine injected the spacecraft into the interplanetary transfer trajectory. During the coasting period, M2020 sent telemetry indicating that the Cruise stage was power-positive. Spacecraft separation took place ~4.7 min after this second burn once the Centaur spun up M2020 to ~2 RPM and maneuvered into the spacecraft separation attitude. Launch event time variability for a given launch opportunity was important to ensure initial acquisition of the spacecraft. The average 3-sigma dispersion for the spacecraft separation time event across all launch days was ± 12 s. Figures 5 and 6 show the launch of M2020 on an Atlas V 541 and the M2020 flight system moments after separation as viewed from the Centaur upper stage respectively.

The flight performance of the launch vehicle was outstanding and the M2020 spacecraft separated only ~2.8 s later than the nominal time. Table 2 shows the expected vs. the actual event time from Go-Inertial command to spacecraft separation. The launch of the M2020 spacecraft marked the 84th Atlas V launch and the 255th Centaur launch.



Figure 5. Liftoff of the Atlas V carrying M2020 Perseverance (Credit: NASA/ULA)



Figure 6. Spacecraft Separation as viewed from the Centaur Upper Stage (Credit: NASA/ULA)

Table 2. Planned vs. Actual Launch Vehicle Time Events

Event	Mission Elapsed Time (MET)			Delta(sec)
	Expected Time (sec)	Actual Time (sec)	Actual Time (min:sec)	
Actual T-Zero Time: 30-Jul-2020 11:50:00 UTC				
Guidance Go-Inertial	-7.96	-7.96	-00:07.96	0.000
T-Zero	0.00	0.00	00:00.00	0.000
Liftoff (T/W > 1)	1.07	1.07	00:01.07	0.000
Solid Rocket Booster Jettison #1 and #2	109.44	109.39	01:49.39	-0.050
Solid Rocket Booster Jettison #3 and #4	110.94	110.89	01:50.89	-0.050
Payload Fairing Jetisson	208.22	207.10	03:27.10	-1.120
BECO	262.82	262.44	04:22.44	-0.380
Atlas/Centaur Separation	268.82	268.43	04:28.43	-0.390
MES-1	278.80	278.40	04:38.40	-0.400
MECO-1	689.26	683.42	11:23.42	-5.840
Burn-1 Duration	410.46	405.02	06:45.02	-5.440
Park Orbit Coast Duration	2011.08	2014.72	33:34.72	3.640
MES-2	2700.34	2698.14	44:58.14	-2.200
MECO-2	3170.56	3167.40	52:47.40	-3.160
Burn-2 Duration	470.22	469.26	07:49.26	-0.960
M2020 Separation	3453.26	3450.46	57:30.46	-2.800

Notes:

- T/W = Thrust/Weight ratio. BECO = Booster Engine CutOff. MES-1 = Main Engine Start #1.

MES-2 = Main Engine Start #2. MECO-1 = Main Engine CutOff #1; MECO-2 = Main Engine CutOff #2

LAUNCH INJECTION ACCURACY

The M2020 launch targets (C3, DLA, and RLA) at the Targeting Interface Point (TIP) were generated using open-loop entry trajectories targeted to Jezero Crater located at 18.4° N and 77.5° E. Jezero Crater was used as the trajectory target for all target specifications even before its final selection because it was the highest ranked site and the ΔV cost of retargeting to any of the other original candidate landing sites which included NE Syrtis (17.9° N, 77.2° E), and Columbia Hills (14.6°S, 175.4°E) was minimized with respect to the rest of the candidate sites⁴. Note that even though the exact target inside Jezero target shifted over time, for the purposes of the target specification, its location remained unchanged from early on in the target specification process since these launch targets were biased to be in compliance with planetary protection regulations and any changes to the final landing target would be corrected by planned trajectory correction maneuvers (TCMs).

The targets were delivered to ULA in the form of launch polynomials with the independent variable being the time in minutes measured from the optimal launch time. The launch targets also satisfied two planetary protection requirements: (1) The probability of impact of Mars by the launch vehicle shall not exceed 1.0×10^{-4} , and (2) the probability of non-nominal impact of Mars due to failure during the cruise and approach phases shall not exceed 1.0×10^{-2} . This was achieved by biasing the injection aimpoint and using Trajectory Correction Maneuvers (TCMs) during cruise to remove the injection bias. Due to an outstanding injection imparted by the Centaur and small maneuver execution and orbit determination errors, a combined TCM-1/-2/-3 optimization strategy was able to remove all the injection biasing and target to the desired EIP.

The launch energy (C3) increased from $\sim 13.8 \text{ km}^2/\text{s}^2$ on July 23, 2020 to a maximum value of $\sim 20.7 \text{ km}^2/\text{s}^2$ at the close of the launch period. The DLA ranged from a minimum value of ~ 13.8 deg at the close of the launch window to a maximum value of ~ 35.3 deg on July 17, 2020. Table 3 shows the target conditions for the open, middle, and close of the launch window for each launch day. The targets assume a

spacecraft mass of 4,102 kg. Due to the high DLA at the open of the launch period, two park orbit families were used, (1) a “High” park orbit inclination of 34.6 deg for launch dates from July 17, 2020 through July 23, 2020 and (2) a “Low” park orbit inclination of 29.1 deg for launch dates from July 24, 2020 through August 15, 2020. Note that the targets were specified at the Target Interface Point (TIP), which was defined at spacecraft separation plus 240 s.

Table 3. Launch Targets

		Earth Centered EME2000 Coordinates (C3, DLA, RLA) at TIP									
	Launch Day	Launch Date (2020)	C3 (km²/s²)			DLA (deg)			RLA (deg)		
			Open	Middle	Close	Open	Middle	Close	Open	Middle	Close
Launch Days eliminated due to delays in LV Readiness	-	07/17	14.4813	14.4648	14.4519	35.3378	35.2602	35.2065	13.9553	13.9560	13.9583
	-	07/18	14.2798	14.2650	14.2503	34.3086	34.2324	34.1644	13.7033	13.7010	13.7012
	-	07/19	14.1167	14.1020	14.0881	33.3056	33.2218	33.1493	13.4093	13.4038	13.4005
	-	07/20	13.9870	13.9745	13.9659	32.3006	32.2206	32.1674	13.0791	13.0706	13.0655
	-	07/21	13.8948	13.8877	13.8792	31.3205	31.2679	31.2012	12.7217	12.7139	12.7037
	-	07/22	13.8388	13.8331	13.8273	30.3626	30.3121	30.2492	12.3442	12.3346	12.3217
	-	07/23	13.8174	13.8131	13.8100	29.4264	29.3778	29.3184	11.9536	11.9426	11.9272
	-	07/24	13.8347	13.8319	13.8301	28.6084	28.5474	28.5065	11.5688	11.5566	11.5501
	-	07/25	13.8758	13.8745	13.8741	27.7294	27.6619	27.6164	11.1712	11.1559	11.1474
	-	07/26	13.9457	13.9460	13.9474	26.8658	26.8066	26.7505	10.7733	10.7582	10.7457
	-	07/27	14.0429	14.0451	14.0482	26.0223	25.9587	25.9119	10.3778	10.3600	10.3480
	-	07/28	14.1661	14.1702	14.1744	25.1988	25.1383	25.0998	9.9854	9.9667	9.9557
	-	07/29	14.3137	14.3195	14.3252	24.4025	24.3450	24.3089	9.5984	9.5787	9.5674
Available Launch Days	1	07/30	14.4844	14.4919	14.4990	23.6328	23.5781	23.5442	9.2163	9.1958	9.1843
	2	07/31	14.6772	14.6827	14.6937	22.8889	22.8524	22.8092	8.8386	8.8243	8.8069
	3	08/01	14.8918	14.8982	14.9110	22.1700	22.1350	22.0944	8.4649	8.4501	8.4325
	4	08/02	15.1293	15.1357	15.1486	21.4699	21.4425	21.4080	8.0923	8.0795	8.0629
	5	08/03	15.3894	15.4008	15.4098	20.7960	20.7621	20.7429	7.7225	7.7041	7.6945
	6	08/04	15.6731	15.6842	15.6942	20.1514	20.1246	20.1067	7.3534	7.3371	7.3270
	7	08/05	15.9789	15.9914	16.0001	19.5479	19.5231	19.5098	6.9793	6.9623	6.9532
	8	08/06	16.3061	16.3194	16.3286	18.9810	18.9575	18.9444	6.5663	6.5463	6.5350
	9	08/07	16.6499	16.6618	16.6717	18.3678	18.3448	18.3284	6.0772	6.0591	6.0480
	10	08/08	17.0227	17.0363	17.0475	17.6613	17.6383	17.6224	5.6674	5.6538	5.6462
	11	08/09	17.4410	17.4533	17.4656	17.0028	16.9870	16.9734	5.3509	5.3409	5.3338
	12	08/10	17.8909	17.9042	17.9141	16.4094	16.3948	16.3852	5.0495	5.0393	5.0333
	13	08/11	18.3766	18.3874	18.3980	15.8449	15.8347	15.8256	4.7454	4.7377	4.7318
	14	08/12	18.8930	18.9045	18.9160	15.3061	15.2963	15.2875	4.4485	4.4409	4.4350
	15	08/13	19.4473	19.4577	19.4679	14.7839	14.7762	14.7691	4.1589	4.1533	4.1485
	16	08/14	20.0401	20.0489	20.0576	14.2794	14.2734	14.2679	3.8830	3.8785	3.8747
	17	08/15	20.6755	20.6802	20.6849	13.7909	13.7880	13.7853	3.6212	3.6192	3.6173

Historically, planetary missions have used a variety of methods to assess injection accuracy. A commonly used method simply compares the actual C3, DLA, and RLA errors to the individual maximum allowable values or tolerances. Other methods would evaluate the magnitude of the post-launch ΔV to target to the desired atmospheric entry aimpoint or to target back to the desired biased injection point and compare them to the maximum allowable values. These methods are commonly used for orbiter missions that carry large propellant margins or spacecraft that use planetary flybys or large Deep Space Maneuvers (DSM), which can offset a significant amount of the injection error⁷. M2020, just like InSight and MSL, carried a limited amount of cruise propellant, which translated into a potentially small cruise propellant margin; hence, a large cruise ΔV required to correct injection errors could have been catastrophic. In order to account for the effects of injection errors on cruise propellant usage, MSL developed an error ellipsoid probability method that included the effects of injection errors mapped to the Mars B-plane by accounting for corrections of C3, DLA, and RLA errors and worst-case cruise propellant usage at the 99.0% probability level (3.36 σ for a 3-dimensional distribution). This method was dependent on the Injection Covariance Matrices (ICMs) and accounted for effects of injection errors on Mars impact probability in order to satisfy planetary protection requirements. MSL’s error ellipsoid method was subsequently updated slightly by InSight so mission success was based on ICMs scaled up to the Figure of Merit requirement instead of using the unscaled ICMs developed for the design of the injection aimpoints. The Figure of Merit for M2020, a measure of TCM

performance to correct injection errors, was 5.0 m/s. Table 4 shows the injection accuracy results in terms of C₃, DLA, and RLA at TIP in EME2000 coordinates, the 1 σ uncertainties based on the M2020 Navigation Team's orbit determination solution, expected 1 σ dispersions, and the sigma levels of the errors with respect to the expected 1 σ dispersions. The expected dispersions were derived from the ICM for a launch on July 30, 2020 at the launch window open (T-Zero = 11:50:00 UTC). Note that the small differences in the launch targets between Table 3 and Table 4 are due to updated launch window open and close times between the final launch vehicle target spec cycle and ULA's official launch windows memo released a few weeks prior to launch⁶.

Table 4. Injection Accuracy Assessment

Parameter	Achieved	Target	Error	OD Uncertainty (1 σ)	Expected Dispersion (1 σ)	Error σ Level
TIP Epoch		30-Jul-2020 12:51:30.12 UTC				
C ₃ (km ² /s ²)	14.4822	14.4866	-0.0043	9.54E-07	±0.0231	-0.19 σ
RLA* (deg)	9.2099	9.2090	0.0009	8.13E-06	±0.0487	0.02 σ
DLA* (deg)	23.6153	23.6131	0.0022	1.56E-05	±0.0252	0.09 σ

*EME2000 coordinate system.

Error sigma level: $(n \sigma)^2 = dx^T \cdot C^{-1} \cdot dx$

where: C is the 3x3 covariance matrix and dx is the (achieved targets - nominal targets) (3x1 matrix)

With respect to the principal axis injection error ellipsoid defined by the injection covariance matrix, the C₃, RLA, and DLA injection errors listed in Table 4 correspond to a 0.27 σ error or, equivalently, a 0.512% error probability level. These values indicate that the launch targets were achieved with great accuracy, easily satisfying the 3.36 σ injection accuracy requirement for launch vehicle mission success. For reference, injection errors of 0.79 σ or 10.9% error probability level were estimated using the unscaled 3x3 Injection Covariance Matrix⁸.

MARS B-PLANE PARAMETERS

The injection errors propagated to the Mars B-plane in terms of B•R, B•T, and Time of Closest Approach (TCA) are shown in Table 5. The targets were obtained by propagating the TIP state included in the Near-Earth Trajectory Space (NETS) files provided by the launch vehicle provider to the Mars B-plane. The achieved values and 1 σ uncertainties were based on the M2020 Navigation Team orbit determination solution. The expected 1 σ dispersions were derived from the ICM for a launch on July 30, 2020 at the launch window open (T-Zero = 11:50:00 UTC) propagated to the Mars B-plane. The B•R, B•T parameters are expressed in the Mars Mean Equator and Equinox of Epoch reference frame⁸.

Table 5. Injection Errors Mapped to the Mars B-Plane

Parameter	Achieved	Target	Error	OD Uncertainty (1 σ)	Expected Dispersion (1 σ)	Error σ Level
B.R* (km)	27,983.372	15,548.798	12,434.574	608.219	73,711.412	0.169
B.T* (km)	52,350.958	43,758.598	8,592.360	657.654	31,841.743	0.270
TCA** (19-Feb-2021 02:55:09.41 UTC)	10,438.070	0.000	10,438.070	363.975	53,278.883	0.196

*Mars Mean Equator IAU Node of Date Inertial IAU 2000. **TCA = Time of Closest Approach.

SEPARATION ACCURACY ASSESSMENT

The spacecraft separation attitude and angular rates targets were fixed across the launch period. This separation was defined as the instant of loss of contact between the spacecraft and the separation system hardware on the Centaur upper stage.

Table 6 shows the separation accuracy results in terms of the right ascension and declination of the spacecraft -Z-axis in EME2000 coordinates, and spacecraft spin rate (positive about the +Z axis). The

estimated values were based on post-separation spacecraft telemetry. The achieved separation conditions in terms of spacecraft attitude and spin rate following separation from the Centaur upper stage were very close to the desired values; hence, satisfying the separation accuracy requirements. This table also shows the spacecraft separation requirements. Note that the spacecraft separation attitude error included nutation effects and spacecraft wobble effects that could manifest after spacecraft. The trans-Mars injection and Spacecraft separation provided by the Centaur were outstanding setting a new standard on launch vehicle performance. separation but prior to any spacecraft propulsive maneuvers⁸

Table 6: Separation Accuracy Assessment

Parameter	Estimated	Desired	Error	Estimate Uncertainty (99%)	Required Accuracy
SEP Epoch	30-Jul-2020 12:47:30 UTC				
'+Z _{SC} Axis Right Ascension ^{1,3,4} (deg)	306.592	306.55	0.042	-	-
'+Z _{SC} Axis Declination ^{1,3,4} (deg)	23.353	22.96	0.393	-	-
Total Attitude Error ⁴ (deg/s)	-	-	0.395	1.2	< 8.0
Spin Rate ^{2,5} (deg/s)	15.024	15	0.024	0.02	± 3.0

¹EME2000 coordinates. ²Positive about +Z axis. ³Positive about angular momentum (+H) vector. ⁴Computed on 07/31/20 at 18:49 UTC.

⁵Computed on 07/30/20 at 22:03 UTC.

DSN INITIAL ACQUISITION

Spacecraft telemetry was interleaved with launch vehicle telemetry, transmitted to the ground through the Tracking Data Relay System (TDRS) and available from launch through spacecraft separation. Upon completion of the second Centaur injection burn and following a wait time of ~283 s, pyrotechnic actuators and push-off springs on the launch vehicle released the spacecraft with a separation velocity of 0.11 m/s, and a pointing attitude and angular rates discussed in the previous section. Spacecraft separation was one of the most critical events of the mission since it marked the first time the spacecraft communicated directly to the Deep Space Network (DSN) antennas via its low-gain antenna. This was achieved by turning on the spacecraft's Travelling Wave Tube Amplifier (TWTA), which powered the transmitter on.

On MSL, shadowing from the Earth was not a concern since only a few trajectories had any solar eclipses and for those singular events, eclipses only lasted for a few minutes⁹. On M2020, the spacecraft could have spent anywhere between 25 and 46 min being occulted from the Sun and between 10 and 42 min in solar eclipse after spacecraft separation¹⁰. For the actual launch trajectory, total eclipse duration was ~31 min and eclipse duration after separation was about ~21 min. Due to power constraints after launch vehicle separation and while inside solar eclipse, a delay in initial acquisition was warranted for all launch opportunities. Once the eclipse timer based on the estimated eclipse exit time expired, the spacecraft transitioned to cruise mode. At that point, spacecraft cruise configuration tables were executed, the TWTA was powered on about 1 min and 16 sec later, and transmission started after a warm-up period of 4 min and 54 sec. Note that based on pre-launch testing, the spacecraft radio reached a ready-to-transmit time within a few seconds from the expected time. Figure 7 shows the departure geometry with its long occultation after MES-2. Figure 8 illustrates the ground track along with the main launch vehicle events and initial ground station rise/set times from launch through MECO-1 plus 24 hours.

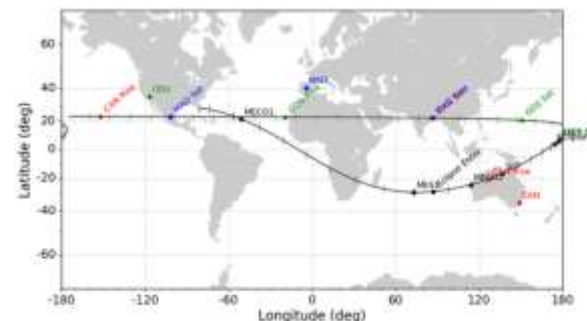
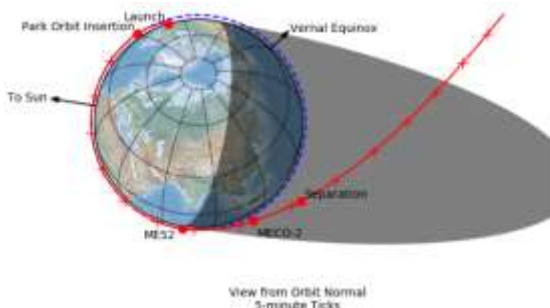


Figure 7. Departure Geometry **Figure 8. Ground track** **SS-34 and DSS-36 served as prime uplink/downlink and backup uplink/downlink respectively.** Stations at Goldstone Deep Space Communications Complex (GDSCC), DSS-24 and DSS-25 provided concurrent support as backup uplink/downlink to Canberra. Both CDSCC and GDSCC had DSN level-1 support to ensure committed data services would be provided as required. Stations were supported by Madrid and Goldstone personnel in accordance to the Follow-the-Sun paradigm¹¹. DSN stations were preconfigured with an open loop receiver set to the cruise nominal downlink rate of 2 kbps and with a backup receiver set to the safe mode downlink rate of 40 bps. DSS-36 locked on the carried signal as expected at 13:15:24 UTC and locked on telemetry at 2 kbps for a few seconds at 13:16:18 UTC but then lost lock. The concurrent station primary receiver at GDSCC locked on telemetry but only the primary station was set to flow data directly to mission control at JPL. At short Earth distances, it was known that the TWTA transmitter would likely saturate the DSN receiver; hence, a 20 dB attenuator was installed; however, that was not sufficient to acquire the signal. Swedish Space Corporation (SSC) stations supported the launch in case of a contingency and collected some telemetry during this anomaly. In that data, SSC reported a bit rate change which was an indication of a possible safe mode entry shortly after locking telemetry at the expected nominal rate of 2 kbps. Meanwhile the DSN reconfigured the primary receiver and the antenna for safe mode. With the help of off-pointing to avoid signal saturation, solid telemetry was finally acquired by DSS-25 at 15:32:24 UTC (2 hours and 19 min after transmitter on) in the safe mode configuration. DSS-25 was followed by DSS-24, DSS-34, and DSS-36¹². The safe mode entry was due to a stuck open check valve on the spacecraft which allowed Heat and Rejection Coolant System (HRCS) fluid to circulate through an auxiliary pump that was powered off resulting in a reduced system flow rate and a temporary increase in temperature. The safe protection response automatically turned the backup and auxiliary pumps to reach nominal HRCS temperatures. Pump characterization activities during cruise unstuck the check valve and confirmed that the HRCS remained healthy with stable temperatures. At 17:03:22 UTC, DSS-34 successfully radiated the first NO-OP command. The next few commands were uplinked shortly after to complete the safe mode recovery and set the downlink rate to the intended early cruise rate of 10 kbps. At 20:39:50 UTC, DSS-34 successfully acquired range lock. Table 7 summarizes the most relevant event times (expected and actuals) in the DSN initial acquisition timeline.

Table 7. DSN Initial Acquisition Timeline

Event	Expected time from Spacecraft Transmitter ON (hh:mm:ss)	Expected time (hh:mm:ss, UTC)	Actual Time from Spacecraft Transmitter ON (sec)	Actual Time (hh:mm:ss, UTC)	Delta (hh:mm:ss)	Notes
Canberra (DSS-34) Rise	-00:28:24	12:45:26	-	-	-	
Canberra (DSS-36) Rise	-00:28:24	12:45:26	-	-	-	
Spacecraft Separation	-00:26:17	12:47:33		12:47:30	-00:00:03	Actual times based on spacecraft telemetry
Spacecraft Eclipse Exit	-00:05:00	13:08:51		13:08:53	00:00:02	Actual times based on spacecraft telemetry. Start of cruise transition started 0.15 sec after eclipse exit
Spacecraft Ready-To-Transmit	-	13:13:51	-	13:15:03	00:01:12	TWTA started warm-up period per SCFG at 13:10:09 UTC. SCFG completed at 13:15:01 UTC
Canberra (DSS-36) Carrier Lock	TXR ON + 10 s	13:14:01	00:00:21	13:15:24	00:01:23	First station to lock on the carrier
Canberra (DSS-36) Telemetry Lock	CAR LOCK + 20 s	13:14:21	00:01:15	13:16:18	00:01:57	First station to lock on telemetry (2 Kbps)*
Goldstone (DSS-24) Rise	00:03:44	13:17:35	-	-	-	Station remained locked on telemetry from 16:08:31 UTC (40 bps)
Goldstone (DSS-25) Rise	00:03:34	13:17:35	-	-	-	
Goldstone (DSS-25) Telemetry Lock	CAR ON + 20 s	13:18:05	02:17:21	15:32:24	02:14:19	First station to maintain telemetry lock (40 bps)
Canberra (DSS-34) NO-OP	ACQ + 35 min	13:48:51	03:48:19	17:03:22	03:14:31	Station remained locked on telemetry from 16:34:09 UTC (40 bps)
Canberra (DSS-34) Range Lock	NO-OP + 10 min	13:58:51	07:24:12	20:39:15	06:40:24	

* DSS-36 and DSS-34 went in and out of CAR/TLM lock multiple times. DSS-25 was the first station to remain in telemetry lock.

INTERPLANETARY CRUISE AND MARS APPROACH

The Cruise phase started with the first commanding of the spacecraft (NO-OP) following initial acquisition on July 30, 2020 and ended on January 4, 2021 when the spacecraft was 45 days from entry into the Martian atmosphere. The Approach phase immediately followed the Cruise phase and ended when the spacecraft reached the Mars atmospheric entry interface point, 3522.2 km from the center of Mars. Up to six nominal trajectory correction maneuvers (TCMs) were planned during cruise¹³. TCM-1/-2/-3 optimization was used to remove the planetary protection bias, correct launch vehicle injection errors, and clean-up previous TCMs. TCM-3 was designed to target the desired Entry Interface Point (EIP) defined at a radius of 3,522.2 km. Exceptional navigation and maneuver execution performance resulted in TCM-3 being the last TCM needed to meet delivery, knowledge and EDL performance requirements. In flight, the team executed TCM-1 on August 15, 2020, TCM-2 on September 30, 2020, and TCM-3 on December 18, 2020. Figure 9 shows a heliocentric view of the M2020 trajectory and the planned TCM execution dates.

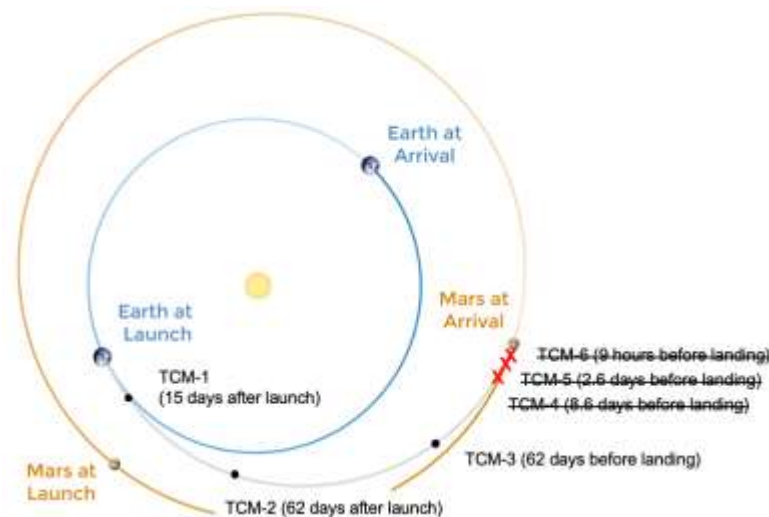


Figure 9. Interplanetary Trajectory

A lateral calibration maneuver executed on August 5, 2020 was used to determine the center of mass offset for the lateral burns and to verify the use of all eight cruise reaction control system (CRCS) thrusters. M2020 completed two engineering checkouts, the first one in late August and the second one in mid-November. Descent stage Inertial Measurement Unit (DIMU) calibrations were successfully executed on October 5-6 and October 12-13, 2020. Two instrument checkouts were executed during cruise, one in mid-October and a second one in early November. The surface flight software was uplinked on December 11-15, 2020. Battery charging activities included: battery discharge from 100% to 50% on August 1, 2020, battery charge from 50% to 100% prior to TCM-1 on August 13, 2020, battery discharge from 100% to 50% after TCM-1 on August 21, 2020, battery charge from 50% to 70% on November 3, 2020, and a final battery charge from 70% to 100% prior to EDL on February 8, 2021. Cold boot activities, designed to format partitions on both Rover Computing Element (RCE) to clear out all old files and data products, and to configure both on-board computers for EDL, were successfully completed on February 1-4, 2021. Nine ACS turns were executed to maintain desired -Z axis off-Sun and off-Earth angles for power, telecommunications, ACS, and thermal constraints during cruise. Helicopter battery recharging activities took place every two weeks approximately. The final helicopter charge activity prior to landing and executed on January 31, 2021 increased the helicopter battery charge to 42.5% which was sufficient to ensure the helicopter's survivability until the first planned battery charging activity on the Martian surface which took place on sol 2. Six Star Scanner Assembly (SSA) and Digital Sun-Sensor Assembly (DSA) calibrations were performed during cruise to calibrate the relative alignment knowledge between the SSA and the DSA. Four Heat Rejection System (HRS) engineering maintenance activities designed to monitor pump pressures, temperatures, and currents were executed. Telecom data transmission rate configurations were updated during cruise following an initial downlink rate of 10K and an uplink of 2K following separation from the Centaur upper stage. On September 5, 2020, the Communications Behavior Manager (CBM) was updated to 5K downlink. CBM was updated to 3.125K downlink on September 22, 2020 and to 1.25K downlink and 1K

uplink on September 28, 2020. Following the transition from the Low-Gain Antenna (LGA) to the Medium Gain Antenna (MGA) on October 14, 2020, CBM was updated to 25K downlink and 2K uplink, 10K downlink on November 17, 2020, 5K downlink on December 14, 2020, and 2K on January 22, 2021. A final uplink update to 1K for EDL was completed on February 5, 2021.

TRAJECTORY CORRECTION MANEUVER PERFORMANCE

Two 19-in diameter tanks were loaded with 72.1 kg of hydrazine propellant. Axial burns were accomplished by firing pairs of axial thrusters continuously for a determined period of time. Lateral burns imparted a ΔV approximately normal to the Z-axis by firing all four thrusters in each cluster for 5 s at the appropriate orientation during each spacecraft revolution, resulting in two 5 s lateral pulses per revolution with one of the axial thrusters firing during a smaller interval in order to ensure that the thrust vector went through the center of mass of the spacecraft. The average Isp values for axial and lateral TCMs were 215.6 s and 227.1 s respectively. These values include blowdown effects and are adjusted to account for thruster plume impingement losses of 6% for axial burns and 1% for lateral burns. During interplanetary cruise, up to six TCMs and TCM-5X, a backup maneuver to TCM-5, were planned. The first three TCMs occurred during the Cruise phase whereas the final three were planned to be executed during the Approach phase. Outstanding navigation and maneuver execution of TCM-3 resulted in cancelation of TCM-4, TCM-5/-5X, and TCM-6. As of the time of this paper, no other Mars lander had ever executed its final TCM with as much time to go prior to EIP (62 days prior to Mars arrival in the case of M2020). TCM-1, TCM-2, and TCM-3 were chained optimized in order to minimize total cruise propellant. TCM-1 was designed to correct injection errors and part of the injection biasing introduced to satisfy the non-nominal impact probability requirement; TCM-2 was designed to correct TCM-1 execution errors and move the biasing aimpoint closer to the desired entry point; and TCM-3 was scheduled to correct TCM-2 execution errors and to target to the desired atmospheric point. Due to the small cruise propellant allocation, good orbit determination solutions and small maneuver execution errors were critical for a precise delivery of the vehicle at the desired atmospheric entry point. Prior to launch, 99% propellant mass estimates were computed across the launch window for each launch day and each launch opportunity to ensure M2020 would have enough cruise propellant to remove launch vehicle errors, aimpoint biasing, and retarget to the desired EIP. Per agreement between the Navigation and the Attitude Control System (ACS) teams, NAV propellant analysis included propellant consumption associated with all TCM burns and only for turns required for implementing TCM-1 (in flight, all TCMs were executed in no-turn vector mode). The maximum propellant allocation for Navigation was 45 kg. Assuming unscaled ICMs, the pre-launch maximum 99% propellant usage was ~26 kg which resulted in a propellant margin of ~42%. Using ICMs scaled-up to the FOM requirement of 5.0 m/s resulted in a 99% propellant usage of ~44 kg. Using scaled-up FOMs for this analysis was deemed as a very conservative approach. If needed, ACS could have released up to 8 kg of propellant for TCMs. Navigation could have also changed maneuver dates and maneuver implementation modes to increase propellant usage margins. Figure 10 shows the 99% propellant mass usage using unscaled ICMs across the launch period. In flight, total propellant consumption for all TCMs and the lateral calibration maneuver was about 9.1 kg (~80% margin)¹⁴.

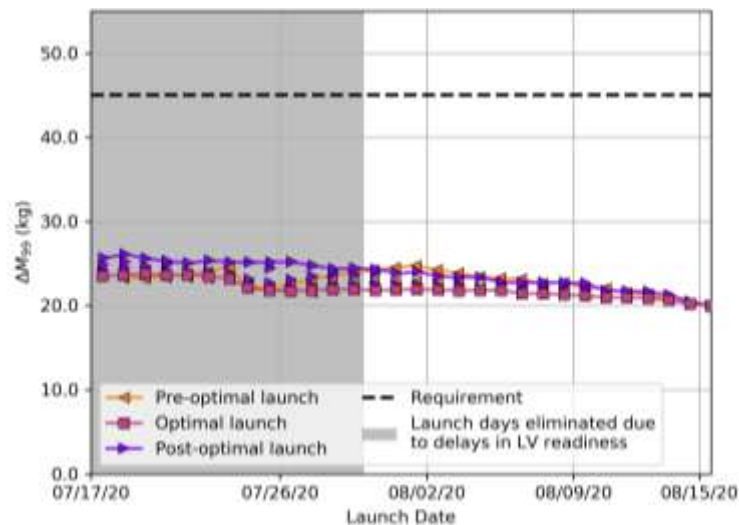


Figure 10. 99% Propellant Mass

The total planned ΔV for TCM-1 through TCM-3 was ~ 2.2 m/s and the total implemented ΔV was ~ 2.9 m/s. The estimated TCM propellant used was ~ 7.8 kg. Maneuver execution errors were very small. The largest magnitude error was 1.6% which corresponded to TCM-2. Pointing errors were less than 1.0 deg. Table 8 shows the pre-launch and actual maneuver dates, planned and implemented ΔV s, estimated TCM propellant usage and maneuver accuracy^{15,16,17}.

Table 8. TCM Maneuver Performance

Event	Pre-Launch Execution Date (2021, UTC)	Actual Execution Date (2021, UTC)	Maneuver Mode	Planned DV (m/s)	Implemented DV (m/s)	Estimated Propellant Usage (kg)	Maneuver Accuracy				
							+Z (%)	-Z (%)	Lateral (%)	Total Magnitude Error (%)	Total Pointing Error (deg)
Lat Calibration	05-Aug	06-Aug	Lateral	0.531	0.531	1.313	-	-	-2.1	-2.1	0.3
TCM-1	14-Aug	15-Aug	Vector	1.887	2.604	6.893	-	3.9	0.9	0.7	0.9
TCM-2	28-Sep	30-Sep	Vector	0.194	0.208	0.537	3.1	-	-0.8	-1.6	0.6
TCM-3	20-Dec	18-Dec	Vector	0.110	0.115	0.352	3.0	-	-1.1	0.4	0.7
TCM-4	09-Feb	Canceled	N/A	-	-	-	-	-	-	-	-
TCM-5/-5X	15-Feb/16-Feb	Canceled	N/A	-	-	-	-	-	-	-	-
TCM-6	18-Feb	Canceled	N/A	-	-	-	-	-	-	-	-

- Planned DV refers to the ideal ΔV which represents the design inertial velocity change in the trajectory and does not reflect losses due to propulsion system inefficiencies, such as thruster cant angle losses and finite burn losses, or particular maneuver implementation modes.
- Implemented DV accounts for thruster cant angle losses (55.6% for axial thrusters and 30.5% for lateral thrusters), lateral ΔV losses due to finite burn arcs (4.7%), vector mode costs, and other maneuver implementation costs dictated by Sun and Earth pointing constraints.
- +Z/-Z/lateral accuracy compares the reconstructed DV vector with the implemented magnitudes of each component whereas total magnitude/pointing error compares the reconstructed DV vector with the planned (ideal) DV.

CRUISE MAINTENANCE ACTIVITY PERFORMANCE

During cruise and approach, several spacecraft cruise maintenance activities that required usage of the cruise propulsion stage were performed. These activities included spacecraft spin down from the spin rate following Centaur separation to the nominal spin rate of 2 RPM on July 31, 2020, eight Attitude Control System (ACS) maintenance turns from October 15, 2020 through February 1, 2021 to maintain good -Z-axis off-Sun and off-Earth angles for the vehicle to remain at a safe attitude for both power and communications, and a final turn to the EDL attitude on February 9, 2021 before cruise stage separation (10 minutes prior to entry) and the turn to entry (9 min prior to entry). An ACS calibration which consisted of 10 spacecraft turns on September 8, 2020 in order to assess residual translation ΔV resulting from spacecraft turns, and a total of four calibrations of the Descent stage Inertial Measurement Unit (DIMU) on October 6-7, 2020 and October 13-14, 2020 were also executed. Total propellant usage for ACS maintenance turns was ~ 1 kg. Each ACS maintenance turn ranged from 0.4 kg (ACS turn #1) to 31 grams (ACS turn #9). Total propellant load was 72.04 kg, (71.32 useable with 0.38 kg trapped in the lines). Remaining propellant at cruise stage separation was 55.9 kg or $\sim 78.4\%$ of the total¹⁷. Figure 11 shows the propellant mass used during cruise.

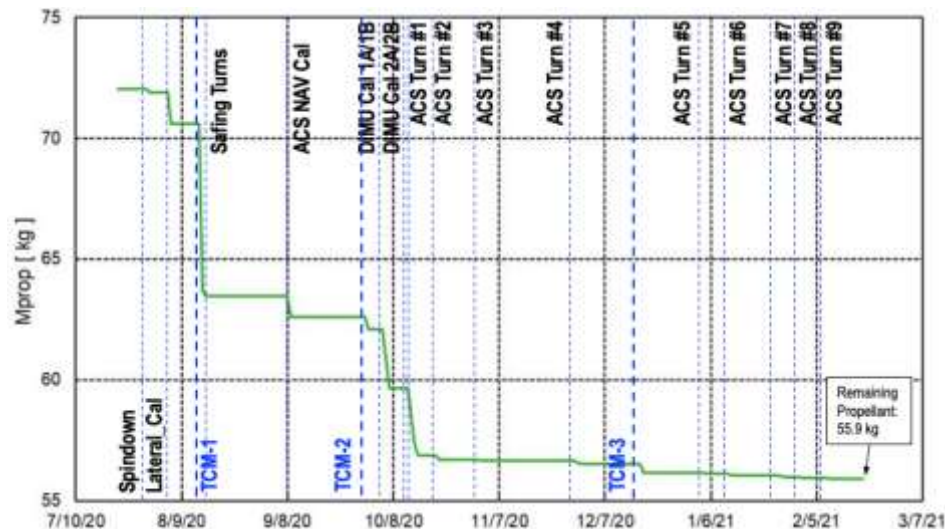


Figure 11. Cruise/Approach Propellant Consumption

ATMOSPHERIC ENTRY DELIVERY AND KNOWLEDGE ACCURACY

Navigation had two key requirements regarding delivery accuracy and knowledge that drove the Trajectory Correction Maneuver (TCM) and EDL Parameter Update (EPU) decision criteria. The combination of orbit determination errors and maneuver execution errors mapped to the atmospheric entry interface point defined the delivery accuracy of each TCM. In order to satisfy the physical constraints of the EDL system and to limit the size of the landing error ellipse, Navigation was required to achieve an Entry Flight Path Angle (EFPA) of -15.5 deg with an uncertainty of ± 0.20 deg and an out-of-plane or cross track error not larger than ± 5 km, all 3-sigma. The atmospheric entry state knowledge (position and velocity) was the Orbit Determination (OD) knowledge accuracy at entry based on an OD data cutoff at Entry minus 6 hours. In terms of knowledge, Navigation was required to provide an inertial state vector at the entry epoch with an accuracy of 2.8 km in position and 2.0 m/s in velocity, all 3-sigma¹⁴. At Nav T0, defined at Entry minus 9 min, the onboard state update criteria were a 0.3 km change in position and 1.0 m/s change in velocity. This state comparison was used as the key and driving criteria to update the onboard state.

Based on a post-landing trajectory reconstruction (OD138) with a Data Cut-Off (DCO) at Entry-50 min using all the data and calibrations leading up to atmospheric entry, the actual Entry Flight Path Angle (EFPA) was well within the 3-sigma requirement being estimated as 0.0166 deg shallower than the -15.5 deg EFPA target. Two EPU files were uplinked to the spacecraft, EPU-1 on February 12, 2021 (Entry minus ~ 5.5 days) and EPU-3 on February 17, 2021 (Entry minus 12 hours). Shortly after the uplink of EPU-1, a *DO_EDL* command was radiated to the vehicle to start the EDL timeline and kick off the vehicle's autonomous behaviors. It is important to note that having an EPU file onboard the vehicle was a prerequisite for the uplink of the *DO_EDL* command. EPU-1 was off by 135 m in position and 0.04 m/s in velocity from the post-landing reconstructed entry state (OD138) at NAV T0.

Comparisons between the onboard state and the latest OD were analyzed through the EPU-4 playcall meeting. Differences between the onboard state and the latest OD solutions were less than the update criteria for each EPU through the EPU-4 playcall meeting held less than 5 hours prior to EDL; nevertheless, the EDL team, in concurrence with the rest of Project key stakeholders, recommended building and uplinking EPU-3 to provide the spacecraft with the best knowledge available at the time of the EPU-3 DCO. The difference between the OD used to generate EPU-3 and EPU-4 DCO was on the order of 14 m in position and 0.004 m/s in velocity; hence, the last opportunity to update the onboard state (EPU-4) was waived. The EPU-3 onboard state was off by 143 m in position and 0.055 m/s in velocity with respect to OD138. The distance between OD138 and the nominal entry target in terms of cross-track was 3.3 km which was well within the delivery requirement. Figure 12 shows the evolution of the Orbit Determination (OD) solutions from the last OD prior to TCM-3 through the last OD solution (OD138). Figure 13 shows the locations of the TCM-3 target, EPU-1 (OD092), EPU-3 (OD112), and the final reconstructed entry state on the B-plane (OD138). The actual locations of these points on the B-Plane are shown in Table 9^{18,19}.

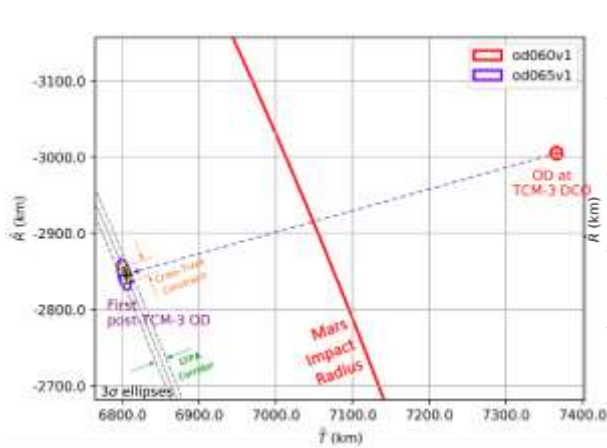


Figure 12. Evolution of OD solutions from last OD prior to TCM-3 through EIP

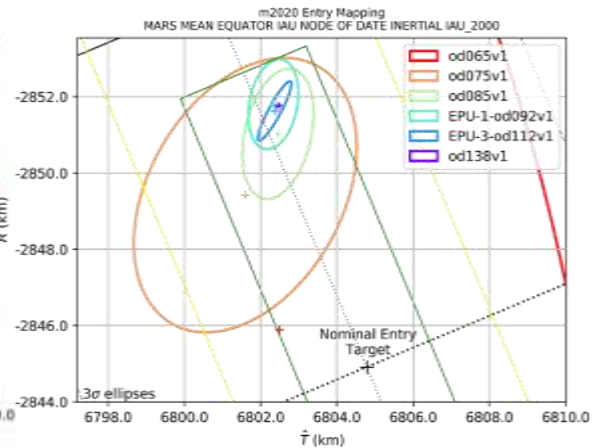


Figure 13. Estimated Entry Points on the B-plane at different Times during Final Approach

Table 9. B-Plane Locations for TCM-3 Target, EPU-1, EPU-3, and OD138

Event	B•R (km)	B•T (km)	DCO (UTC)
TCM-3 Target	-2844.820	6804.720	11-Dec-2020 07:45:00
EPU-1	-2851.800	6802.340	12-Feb-2021 16:30:00
EPU-3	-2851.630	6802.370	18-Feb-2021 00:35:00
OD138	-2851.770	6802.460	18-Feb-2021 20:00:00

EDL ATTITUDE INITIALIZATION

The attitude knowledge requirement for EDL attitude initialization was 0.15 deg (3-sigma) per axis with a goal of achieving 0.1 deg. A comparison of the onboard ACS data to the long-arc despin at the vehicle's final pre-entry attitude showed that the error in the estimated negative-H vector (i.e., the "spin axis") was about 0.023 deg. Including the noise floor of the data, the error in spin phase amounted to 0.03 deg. Initial best estimate of the EDL attitude init during Cruise was 0.08 deg. Preliminary EDL reconstruction analysis indicated an attitude initialization error better than that due to the landing of the vehicle within 5 m of the targeted latitude/longitude.

ARRIVAL GEOMETRY AND EDL COMMUNICATIONS

MRO and MAVEN provided EDL communications support. MRO served as the primary comm path and recorded telemetry in unreliable mode and via its bent pipe capabilities retransmitted the data back to Earth providing near real-time (minus the 11 min and 22 sec one-way light time delay) monitoring of the spacecraft health during EDL. MAVEN recorded the telemetry data stream in open loop. Additional details are provided in the Launch Period and Launch/Arrival Strategy Section since EDL comm was a key driver in the selected launch days and arrival date. An EDL communications overview is shown on Figure 14. Figure 15 illustrates a close-up of the arrival geometry⁵.

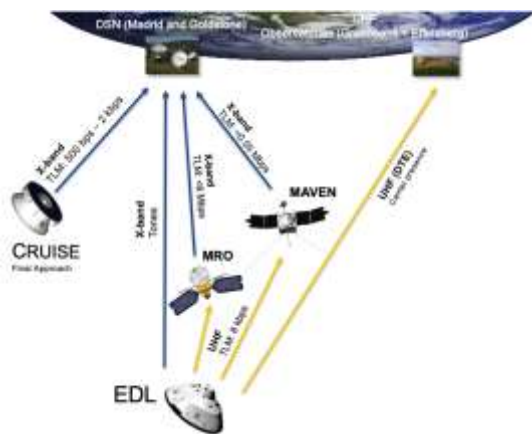


Figure 14. EDL Comm Overview

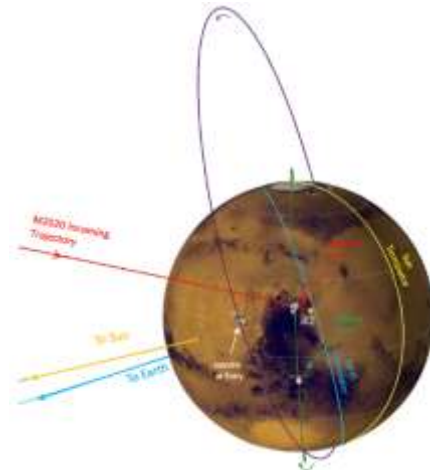


Figure 15. Arrival Geometry

In order to accomplish a successful EDL communications event, the M2020 Navigation team and the orbiters' Navigation teams continuously exchanged trajectory predicts which were evaluated to adjust the requested orbiter positioning as necessary. These targets were specified in the EDL Relay Target Files (ERTFs). The orbiter teams were expected to achieve their EDL relay targets within ± 30 s (MRO), and ± 75 s (MAVEN). Although, ERTF-10 and ERTF-9 specified the final phasing targets for MRO and MAVEN respectively, during each ERTF cycle new targets were generated to compare them with the final ones. The final phasing error was less than -2.0 ± 0.05 sec 3-sigma (MRO) and 10.8 ± 1.7 sec 3-sigma (MAVEN) which was well within the on-orbit phasing requirements for both orbiters^{20,21}. Figures 16 and 17 show the timing phasing offset as a function of date for MRO and MAVEN respectively.

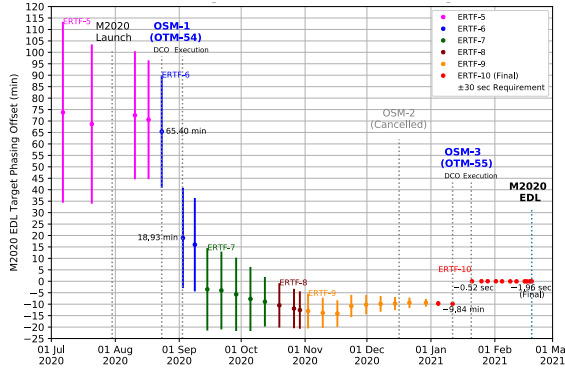


Figure 16. MRO Phasing Offset

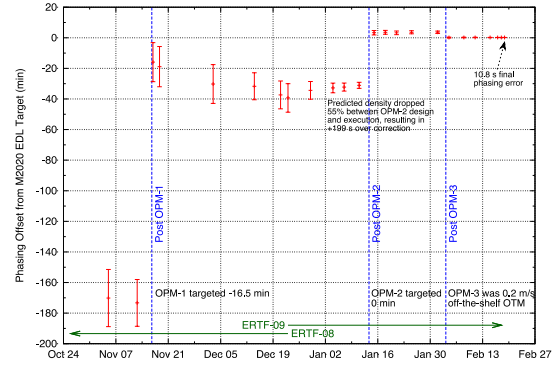


Figure 17. MAVEN Phasing Offset

In flight, MAVEN's recorded EDL open loop data were on the ground within 5 hours from landing and post-processing of the data was completed ~3.5 hours later. In addition to the assets at Mars, the radio telescopes at Green Bank (West Virginia) and Effelsberg (Germany) were configured to detect the UHF signal. Green Bank and Effelsberg detected carrier from Entry through ~43 sec prior to landing (20:54:28 ERT UTC). DTE signal during final descent was not expected due to unfavorable geometry at low altitude. The last observed X-band DTE signal on the open loop receiver was at 20:54:33 ERT UTC²².

EDL TRAJECTORY PERFORMANCE

The performance of the EDL vehicle was outstanding. The pre-launch landing uncertainty was between -43 s and +56 s but the actual EDL events times occurred within 8 s from the predicted EDL event times based on the latest orbit determination solution (OD138)²¹. This landing time uncertainty remained the same as it was primarily a function of altitude at parachute deploy and parachute aerodynamics. The Navigation orbit determination was updated as the vehicle approached Mars but that only shifted the mean time of landing and not the actual landing uncertainty. Table 10 shows the predicted/nominal EDL event timeline and the actual values.

Table 10. Predicted Vs. Actual EDL Event Timeline

Event Name	Predicted (Based on OD138) ^a				Actuals ^a				Delta (s)	Actual Spacecraft Event Time (02/18/2021, PST)	Actual Earth Received Time (02/18/2021, PST)
	Time from Entry (s)	Time from Landing (s)	Altitude (m)	Mars Relative Velocity (m/s)	Time from Entry (s)	Time from Landing (s)	Altitude (m)	Mars Relative Velocity (m/s)			
Entry Interface Point	0.0	-411.1	127,094.2	5,333.5	0.0	-418.8	126,427.9	5,333.1	0.0	12:36:50.1	12:48:12.3
Guidance Start	54.9	-356.1	54,144.0	5,359.6	50.9	-367.9	58,607.6	5,353.9	4.1	12:37:40.9	12:49:03.2
Heading Alignment	139.4	-271.7	14,318.4	1,099.0	139.5	-279.3	14,781.9	1,098.9	-0.1	12:39:09.6	12:50:31.9
Begin SUFR	223.8	-187.3	12,905.8	474.3	223.6	-195.1	13,792.4	487.5	0.1	12:40:33.7	12:51:56.0
End SUFR	237.5	-173.6	11,699.9	428.8	237.6	-181.1	12,509.8	442.0	-0.1	12:40:47.7	12:52:10.0
Parachute Deploy	240.8	-170.3	11,259.5	418.5	240.6	-178.1	12,240.2	433.0	0.2	12:40:50.7	12:52:13.0
Heat Shield Separation	261.2	-149.8	9,554.5	158.5	263.5	-155.2	10,350.7	158.7	-2.3	12:41:13.6	12:52:35.9
TDS Data Start	266.0	-145.1	9,324.5	145.3	268.3	-150.5	10,081.0	142.5	-2.3	12:41:18.3	12:52:40.6
Backshell Separation [*]	349.9	-61.1	2,149.1	80.1	357.5	-61.2	2,179.1	81.1	-7.6	12:42:47.6	12:54:09.9
Earth Occultation	380.0	31.1	-	-	380.6	-38.1	-	-		12:43:10.7	12:54:33.0
Rover Separation	394.7	-16.4	21.3	0.7	402.2	-16.6	30.9	0.8	-7.5	12:43:32.2	12:54:54.5
Touchdown	411.1	0.0	9.2	0.7	418.8	0.0	18.9	0.6	-7.7	12:43:48.8	12:55:11.1

^a Predicted altitude and velocity measured with respect to the wet vehicle center of gravity.

^{*} Based on the as-flown timeline and v1.0 of the GNC reconstruction effort (events are measured with respect to the descent stage IMU).

^{*} X-band DTE was temporarily lost at 20:54:13 ERT UTC and recovered for ~8 sec at 20:54:25 ERT UTC. UHF DTE was lost at 20:54:28 ERT UTC.

In order to calculate the predicted event timeline, a Monte Carlo was run in DSENDS^{YY} and the mean data was calculated to determine the time, altitude, and velocity for most of the events. Some of the events were tracked differently in the Monte Carlo and are noted on the table. For these data, a mean from the Monte Carlo could not be extracted, so the data were interpolated from the nominal trajectory run in the Monte Carlo. Spacecraft data were interpreted to provide the actual times, altitudes, and velocities. The spacecraft directly reported out the time that the events, such as pyro firings for heatshield separation, occurred. The spacecraft also stored all of the sensor data, such as from the IMU and TDS, onboard. These data were

retransmitted to Earth within weeks after landing. A best estimated trajectory of the spacecraft state, including altitudes and velocities, were calculated on the ground through this data along with knowledge of the entry and landing locations.

TERRAIN RELATIVE NAVIGATION

Mars 2020 added Terrain Relative Navigation (TRN) to the autopilot to enable landing between landing hazards (slopes, inescapable craters, dune fields, and rocks). This new capability enabled the selection of the Jezero Crater as the landing target for Mars 2020, which otherwise would have been too dangerous to land (without TRN the landing risk due to hazards would have been 20%, with TRN the landing risk was reduced to 0.3%). TRN performed admirably well during EDL leading to a successful landing. The reconstructed landing location was approximately 5 m from the targeted location selected by TRN. Figure 17 shows an orthographic mosaic of Jezero crater. Figure 18 shows the Jezero crater base map with a hazard map overlay coloring indicating the landing hazards. Both figures include the 99%-tile landing ellipse and the Octavia E. Butler landing location²³.

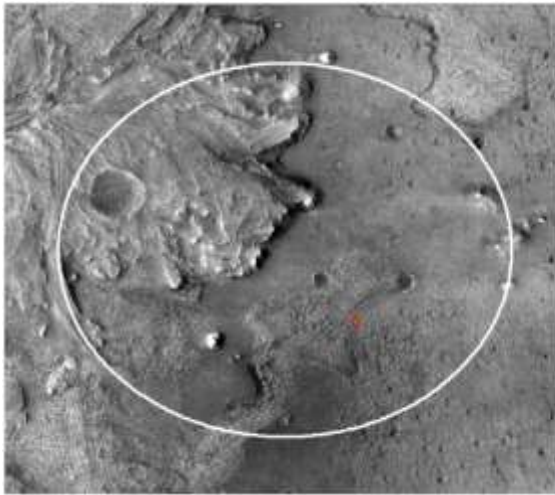


Figure 17. Jezero Crater Orthographic Mosaic

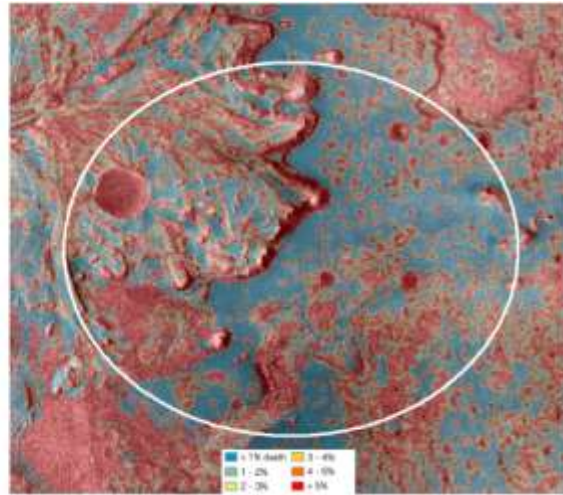


Figure 18. TRN Hazard Map

LANDING ACCURACY

Entry guidance, a technology already used to fly out atmospheric uncertainties on MSL, coupled with the usage of range trigger which deployed the parachute based on range to the target instead of navigated velocity, resulted in a reduction of the M2020 landing errors to 8 km by 7 km which was more than 50% with respect to MSL's. Table 11 shows the coordinates for the target, the coordinates selected by TRN, and the actual landing location using a combination of data sources including local imagery.

Table 11. Target Vs. Achieved Landing Location

Landing Location	Latitude (deg)	Longitude (deg)	Spherical Elevation* (km)	MOLA Elevation^ (km)	Radius (km)
Target	18.4663	77.4298	-4.2370	-2.550	3391.953
TRN Selection	18.4447	77.4508	-4.2530	-2.567	3391.937
Actual	18.4446	77.4509	-4.2530	-2.567	3391.937

*Based on Spherical IAU reference radius = 3396190 m.

^Based on flight CTX DEM radius (v009) - MOLA reference datum radius.

Figure 19 compares the actual landing location with the Monte Carlo predictions based on OD138, as well as the 99%-tile probability ellipses. The overall separation between the target landing site and the achieved target site of ~1.7 km, and the observed landing location is in the 77%-tile relative to the POST OD138 Monte Carlo and in the 79%-tile relative to the DSENDS OD138 Monte Carlo. This separation between target

landing site and achieved target site includes a divert of ~0.6 km away from the target due to safe target selection. The zero divert point at the center of the safe target search wedges is ~1.1 km away from the target landing site. This zero divert point is in the 41%-tile relative to the POST OD138 Monte Carlo and in the 51%-tile relative to the DSEDS OD138 Monte Carlo. The non-gaussian nature of the landing locations is due to TRN diverting to safe landing sites.²⁴

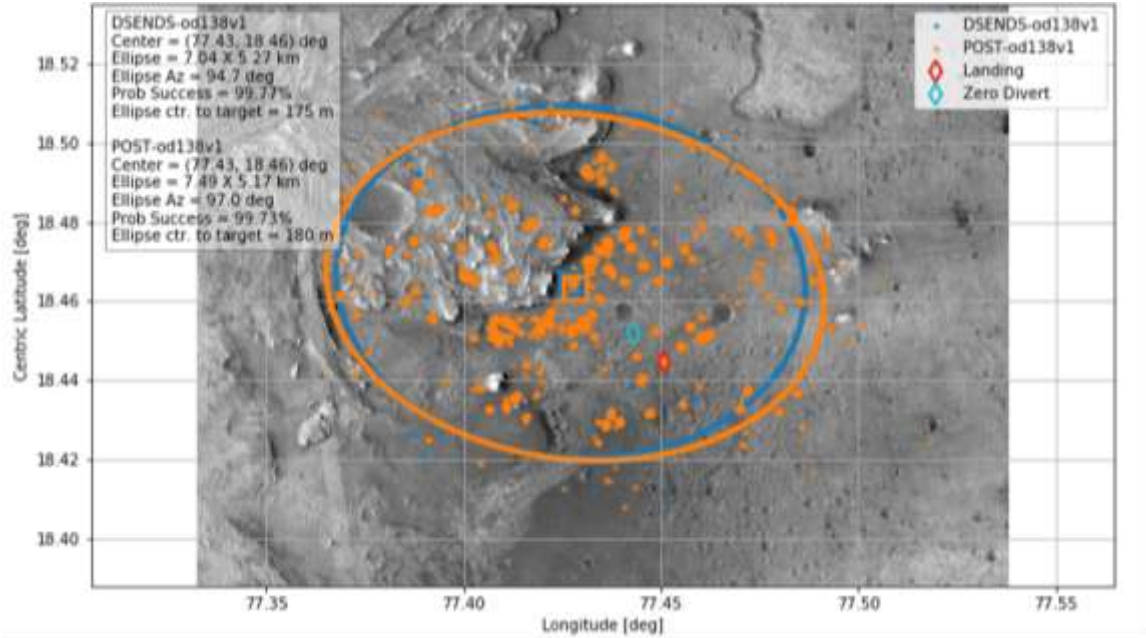


Figure 19. Actual Landing Location and Monte Carlo Predictions from OD138

CONCLUSION

Performance of the Mars 2020 flight system that launched on July 30, 2020 and of all associated assets including the launch vehicle, the Deep Space Network, and the relay orbiters that provided communications during EDL, was nothing short of exceptional. This led to the incredibly successful landing of the Perseverance rover inside Jezero Crater on February 18, 2021 only 1.7 km from the desired target. ULA's Atlas V 541 launch vehicle performance was outstanding with injection errors that amounted to about 0.27σ . DSN provided excellent support and quickly acquired the spacecraft following launch vehicle separation after some needed station reconfiguration. Navigation and maneuver execution performance was extraordinary which resulted in only requiring three Trajectory Correction Maneuvers (TCMs) during cruise with the last maneuver ~62 days prior to Mars arrival. As of the time of this paper, no other Mars lander has ever executed its final TCM with as much time to go prior to entry. Total propellant consumption was less than 8 kg and maneuver execution errors were less than ~2.1%. Both MRO and MAVEN successfully acquired M2020's telemetry after executing a series of maneuvers during the last several years to precisely pre-position themselves to provide EDL communications support from an optimal geometry. M2020's X-band tones were received at the DSN as expected until ~38 sec prior to landing when the local terrain inside the landing region blocked direct-to-Earth communications. UHF direct-to-Earth carrier signal was received as expected at the Green Bank and Effelsberg observatories while geometry was favorable. The addition of range trigger, coupled with the flight-proven guided entry system, significantly reduced the expected landing errors and the Perseverance rover landed ~1.7 km from the landing target. The successful performance of the Terrain Relative Navigation (TRN) system which selected a safe landing location inside the hazard-rich Jezero Crater to maximize the probability of success, was key to a successful landing of the vehicle. Perseverance landed within 5 m from the target selected by the TRN system. The EDL trajectory was nominal with only small timing differences in the event timeline with respect to the nominal trajectory. The landing of the Perseverance rover carrying the most advanced payload suite designed to seek evidence of past life on Mars, which landed in one of the regions that have the most potential to have preserved signs of microbial life, was an out-of-this world achievement and has the potential to rewrite history books.



Mars Perseverance Sol 16: Left Navigation Camera (Credit: NASA/JPL/Caltech)

ACKNOWLEDGEMENTS

The research described in this paper was carried out at the Jet Propulsion Laboratory, California Institute of Technology, under a contract with the National Aeronautics and Space Administration. The author would like to acknowledge Keith Comeaux (Mission Manager), Magdy Bareh (Spacecraft Team Lead); EDL Team members, Aaron Stehura (Deputy EDL Manager), Peter Ilott (Telecomm Lead), Chloe Sackier (EDL Comm Lead), Erisa Stilley (EDL Ops Lead), the members of the M2020 Navigation Advisory Group (NAG), Tomas Martin-Mur (NAG Chair), Erik Bailey, Joe Guinn, Cliff Helfrich, Drew Jones, Tim McElrath, Ralph Roncoli, Roby Wilson, and Tung-Han You; Dave Jefferson (STRATCOM interface); the GNC Technical Advisors Group (GTAG), Miguel San Martin (GTAG Chair), Steve Collins, Gavin Mendeck, and Fred Serricchio; DSN support, Jesse Velasco (Network Operations Project Engineer), Von Petrovic, Sirina Nabhan, and Timothy Hofmann (Network Operations Analysts / Critical Event Planners), Jim Border and Chris Volk (DDOR Analysts), Kamal Oudrhiri (Radio Science Lead), Jarmaine Ollivierre (KSC/Flight Design Analyst), Gaytri Patel (ULA/Flight Design Engineer), and Austin Barrilleaux (ULA/Guidance Engineer).

The author would also like to thank Joe Guinn who served as a reviewer of this paper and provided very helpful feedback.

© 2021 California Institute of Technology. Government sponsorship acknowledged.

REFERENCES

- ¹K. Farley, “Mars 2020 Mission Overview”, Space Science Reviews Volume #216, Article #142, December 3, 2020.
- ²L. Cordero, “Mars 2020 Mass Properties Report”, Revision E, JPL D-98526, June 22, 2020.
- ³F. Abilleira, “2011 Mars Science Laboratory Trajectory Reconstruction and Performance from Launch through Landing”, AAS/AIAA *Space Flight Mechanics Meeting*, February 10, 2013, Kauai, HI.
- ⁴F. Abilleira, “Mars 2020 Project Atlas V 541 Target Specification”, Revision A, JPL D-79385, October 23, 2019.
- ⁵J. Kangas, “Entry, Descent, and Landing Communications for the Mars 2020 Lander Mission”, AAS/AIAA *Astrodynamics Specialist Conference*, August 8-12, 2021, Big Sky, MT.
- ⁶J. Margulies, “AV-088 / Mars 2020 Launch Windows”, ULA-TP-20-053, June 23, 2020.
- ⁷F. Abilleira, “2018 Mars InSight Trajectory Reconstruction and Performance from Launch through Landing”, 29th AAS/AIAA *Astrodynamics Specialist Conference*, January 13-17, 2019, Maui, HI.
- ⁸F. Abilleira, “Mars 2020 Spacecraft Orbit Injection Parameters and Injection Accuracy”, Interoffice Memorandum, M2020-630-20-238, August 6, 2021.
- ⁹F. Abilleira, “Mars Science Laboratory Launch Advisory Handbook”, Revision C (Final), JPL D-68770, MSL-287-3472, March 6, 2012.
- ¹⁰F. Abilleira, “M2020 Project Launch Advisory Handbook”, Initial, JPL D-97362, July 23, 2020.
- ¹¹C. Cagle, “DSN Mission Service Interfaces, Policies, and Practices (MSIPP)”, DSN No. 875-0001, Rev. G, JPL D-26688, February 18, 2015.
- ¹²K. Angkasa, “Critical Event Management Report for Mars 2020 Launch”, IOM 394-KSA-2020730-108, July 30, 2020.
- ¹³J. Gilbert, “Mars 2020 Project Mission Plan”, Revision B, JPL D-79850, March 31, 2020.
- ¹⁴G. Kruizinga, “Mars 2020 Project Navigation Plan”, Revision C, JPL D-95510, December 16, 2019.
- ¹⁵M. Jesick, “Propulsive Maneuver Design for the M2020 Mission”, AAS/AIAA *Astrodynamics Specialist Conference*, August 8-12, 2021, Big Sky, MT.
- ¹⁶S. Wagner, “Maneuver Design Implementation and Verification for the Mars 2020 Mission”, AAS/AIAA *Astrodynamics Specialist Conference*, August 8-12, 2021, Big Sky, MT.
- ¹⁷T. Barber, “Propulsion Mission Ops Trending”, February 19, 2021
- ¹⁸G. Kruizinga, “Mars 2020 Navigation Performance”, AAS/AIAA *Astrodynamics Specialist Conference*, August 8-12, 2021, Big Sky, MT.
- ¹⁹J. Seubert, “Orbit Determination for the Mars 2020 Mission”, AAS/AIAA *Astrodynamics Specialist Conference*, August 8-12, 2021, Big Sky, MT.
- ²⁰P. Menon, “Mars Reconnaissance Orbiter Navigation Strategy for Support of Mars 2020 Mission’s Entry, Descent and Landing Sequence”, AAS/AIAA *Astrodynamics Specialist Conference*, August 8-12, 2021, Big Sky, MT.
- ²¹S. Demcak, “MAVEN Navigation Support of the Mars 2020 Perseverance Entry, Descent and Landing”, AAS/AIAA *Astrodynamics Specialist Conference*, August 8-12, 2021, Big Sky, MT.
- ²²K. Oudrhiri, “Mars 2020 EDL Radio Science Report”, March 19, 2021.
- ²³P. Brugarolas, “[TRN Paper]”, AAS/AIAA *Astrodynamics Specialist Conference*, August 8-12, 2021, Big Sky, MT.
- ²⁴P. D. Burkhart, S. Aaron, C. O’Farrell, “[Mars 2020 Verification Statistical Analysis and Operations]”, AAS/AIAA *Astrodynamics Specialist Conference*, August 8-12, 2021, Big Sky, MT.